The effect of stray fields on Rydberg states in hollow-core PCF probed by higher-order modes

G. Epple,[1,3*] N. Y. Joly[2,1], T. G. Euser,[1,4] P. St.J. Russell[1,2] and R. Löw[3]

[1]Max Planck Institute for the Science of Light and [2]Department of Physics, University of Erlangen-Nuremberg, Staudtstraße 2, 91058 Erlangen, Germany

[3]5. Physikalisches Institut & Center for Integrated Quantum Science and Technology, Universität Stuttgart, Pfaffenwaldring 57, 70550 Stuttgart

[4]NanoPhotonics Centre, Cavendish Laboratory, University of Cambridge, J J Thomson Avenue, Cambridge CB3 0HE, United Kingdom

*Corresponding author: g.epple@mpl.mpg.de

Received XX Month XXXX; revised XX Month, XXXX; accepted XX Month XXXX; posted XX Month XXXX (Doc. ID XXXXX); published XX Month XXXX

The spectroscopy of atomic gases confined in hollow core photonic crystal fiber (HC-PCF) provides optimal atom-light coupling beyond the diffraction limit, which is desirable for various applications such as sensing, referencing and nonlinear optics. Recently coherent spectroscopy was carried out on highly excited Rydberg states at room temperature in a gas-filled HC-PCF. The large polarizability of the Rydberg states made it possible to detect weak electric fields inside the fiber. In this letter we show that by combining highly excited Rydberg states with higher-order optical modes we can gain insight into the distribution and underlying effects of these electric fields. Comparisons between experimental findings and simulations indicate that the fields are caused by the dipole moments of atoms adsorbed on the hollow-core wall. Knowing the origin of the electric fields is an important step towards suppressing them in future HC-PCF experiments. Furthermore, a better understanding of the influence of adatoms will be advantageous for optimizing electric-field-sensitive experiments carried out in the vicinity of nearby surfaces.

OCIS codes: *????????*

http://dx.doi.org/10.1364/OL.99.099999

Introduction The success of electromagnetic induced transparency (EIT) [1] has led to the reestablishment of the spectroscopy of atoms in thermal vapors as an active research field in nonlinear optics. A promising recent approach to optimizing interactions between atoms and the exciting optical field makes use of hollow-core photonic crystal fibers (PCFs) [2], which provide broadband and low-loss guidance of light [3] while enabling incorporation of atomic vapors [4]. The potential of these systems has already been demonstrated in various experiments involving both cold [5] and hot atoms [6-9]. In addition, the latest results on thermal vapors have shown the possibility of creating high optical depths in a controlled manner by making use of light-induced atomic desorption (LIAD) [10,11].

Excitation of Rydberg states makes possible RF and THz-sensing [12,13] and – at higher densities – nonlinear optics, based on mutual interactions between Rydberg atoms [14]. Nonlinear Rydberg interactions between ultracold atoms have already been used to form single photon gates, transistors and subtractors [15-17]. Rydberg interactions can also become dominant in thermal vapors, as has been demonstrated in experiments on Rabi-oscillation damping [18]. Very recently, new phenomena including aggregation effects [19] and bistability [20,21] have been reported. These systems would profit from the increased atom-light coupling and microscale confinement offered by hollow-core PCF.

In previous work we demonstrated the excitation of Rydberg states in a hollow-core PCF filled with thermal cesium vapor [22]. Unexpected level shifts were observed, which we attributed to the presence of dc electric fields in the vicinity of the sub-micron-thick glass core walls, which act on the highly polarizable Rydberg atoms, shifting their energy levels. Measurements on different Rydberg orders, using well-known scaling laws [23], corroborated this view. A better understanding of origin of these level shifts is essential both to find ways to avoid them and to estimate the limitations they place on the accuracy of PCF-based Rydberg spectroscopy in specific applications.

In this Letter we report how the distribution of these stray electric fields can be probed by filling the fiber with Cs atoms, exciting them into a Rydberg state (the sensitivity increases with Rydberg order) and probing the system with guided modes of different order. The probe beam of a three-photon excitation scheme is sent to a spatial light modulator (SLM), where the desired mode profile is synthesized and then launched into the HC-PCF. Different guided mode orders preferentially probe the Rydberg atoms in different regions of the core, providing a degree of spatial resolution.

Experimental implementation Fig. 1 a shows the schematics of the experimental system. An 8-cm-long kagomé-style hollow-core photonic crystal fiber (kagomé-PCF) with core diameter of 60 µm (Fig. 1 b) was mounted in a vacuum system and exposed to cesium vapor for several weeks, so as to obtain sufficient Cs vapor

density inside the fiber. A three-photon excitation scheme involving only infrared light fields was used to excite Cs Rydberg states (Fig. 1 c). The $6S1/2 \rightarrow 6P3/2$ transition at 895 nm served as the probe light field. The intermediate $6P3/2 \rightarrow 7S1/2$ transition and the Rydberg transition $7S1/2 \rightarrow nP3/2$ were excited respectively by 1359 nm light and 790 nm light. The 790 nm beam was guided through a tapered amplifier, giving access to higher intensities and therefore a better coupling strength to the Rydberg state. The three beams were superimposed with dichroic mirrors (DM) and launched into the HC-PCF using achromatic lenses (AL) in a counter-propagating configuration so as to partly compensate for Doppler effects. A typical obtained transmission spectrum is plotted in (Fig. 1 d).

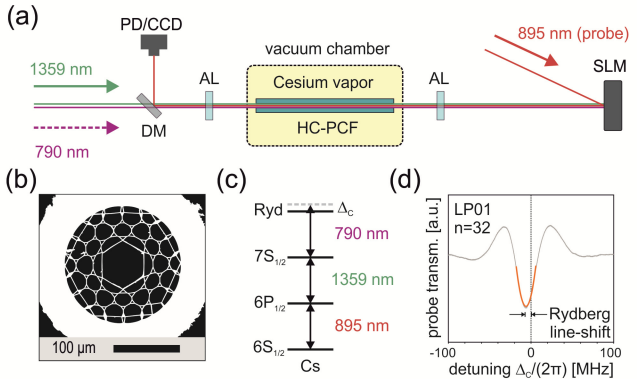

Fig. 1. Schematic of the experimental system: (a) Rydberg atoms are excited in thermal Cs vapor filling a kagomé-PCF. Counter-propagating configuration of the excitation beams. The 895 nm probe beam is launched into different higher-order modes using a spatial light modulator (SLM). (b) Scanning electron micrograph of the investigated kagomé-PCF. (c) Three-photon Rydberg excitation scheme of Cs. (d) Typical obtained three-photon transmission spectrum. The signal position is extracted by a parabolic fit to the absorptive feature.

The 1359 nm and 790 nm beams were coupled into the fundamental LP_{01}-like mode. The 895 nm probe beam was modulated using a spatial light modulator (SLM), enabling controlled excitation of higher-order optical modes [24]. Fig. 2 (upper row) shows the near-field intensity profiles of the 895 nm light for the experimentally excited LP_{01}, LP_{11} and LP_{31} modes, obtained by imaging the fiber end using a CCD-camera. The launch efficiencies were 57% (LP_{01}), 40% (LP_{11}) and 12% (LP_{31}) for the 895 nm probe light, 38% (LP_{01}) for the 1359 nm light and 58% (LP_{01}) for the coupling light. The powers were set to 12.4 µW (1359 nm), 18.9 mW (790 nm) and 0.16 µW (895 nm, all modes), measured at the fiber output. To assure steady state measurement conditions the light fields are launched in the fiber several hours before the data is taken.

For the Rydberg spectroscopy, the 895 nm and 1359 nm diode lasers were frequency-locked (stability ~1 MHz) to a reference cell. The transmitted 895 nm probe signal was measured using a photodiode while the 790 nm excitation light was scanned in frequency over the chosen Rydberg line. The 790 nm beam with the highest power was square-wave-modulated using an acousto-optic modulator, allowing use of a lock-in amplifier. This modulation was also important for preventing density changes during the measurements due to light induced atomic desorption (LIAD). Recent experiments have revealed two different timescales for LIAD and shown that the process is dominated by the average power [10,11]. We found that modulating the 790 nm beam at 15 kHz provided an approximately constant optical depth optical depth of OD=0.8 in our HC-PCF system. All the experiments were performed at room temperature (~23°C), yielding in an atomic density low enough to exclude mutual interactions between Rydberg atoms while minimizing the creation of free Cs ions in the fiber core. The influence of core-confinement was probed by comparing, for a series of different $nP_{3/2}$ Rydberg states, the spectroscopy signal obtained in the kagomé-PCF with simultaneous measurements in a reference cell. The frequency of each signal was extracted by fitting the narrow absorption peak within the transmitted spectrum (Fig. 1 d) [22]. The measurements were performed for three different optical modes (Fig. 2), giving access to different average distances between the probed atoms and the core walls and hence to radial information on the electric field distribution.

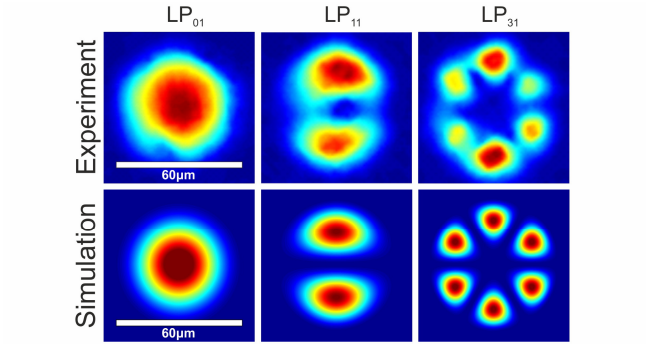

Fig. 2. Near-field intensity profiles of the LP_{01}, LP_{11} and LP_{31} modes in the experiment (top row, measured using a CCD camera) and in simulations using the capillary approximation (bottom row).

Results & simulations The main experimental results are shown in Fig. 3. The data-points show the average measured frequency shifts of the Rydberg absorption over a series of different principal quantum numbers n and spatial modes of the probe light field. The error-bars include uncertainties in lock-in amplifier delay, in scaling the frequency axis and in fitting the line-centers. As described above, the Rydberg states are probed by three different optical fiber modes: LP_{01} (black squares), LP_{11} (red diamonds) and LP_{31} (purple circles). To compensate for electronic delays between fiber and reference-cell measurements, the y-axis is offset by –1.5 MHz. A clear red-shift of the signal is observable for all modes, increasing with principal quantum number n and with mode order (higher orders probe closer to the core-wall). We attribute this shift to a Stark energy shift $\Delta\mathcal{E} = -\alpha E^2/2$ (where E is the electric field and α the atomic polarizability) of the Rydberg state due to a constant electric background field. We therefore expect δ to scale with the atom polarizability $\alpha \sim (n^\star)^7$, where $n^\star = n - \delta$ is the effective main quantum number, given by the principal quantum number n and the quantum defect for cesium, $\delta = 3.558$ [25]. In the following we will only consider the scalar polarizability of the atoms, neglecting the tensor contribution, which is at least an order of magnitude smaller [26]. Fitting a $(n^\star)^7$ scaling law to the data (black lines in the log-log inset in Fig. 3) yields good agreement with the electric field assumption and previous observations [22,27].

One must keep in mind, however, that line-shifts can be caused by other effects, such as Rydberg-Rydberg interactions or Casimir-

Polder potentials. While Rydberg-Rydberg interactions have been observed in thermal systems [18], the Rydberg density in our system is orders of magnitude too low for this interaction to be relevant. Furthermore, Rydberg-Rydberg interactions should not depend on the launched optical mode, in contrast to our findings.

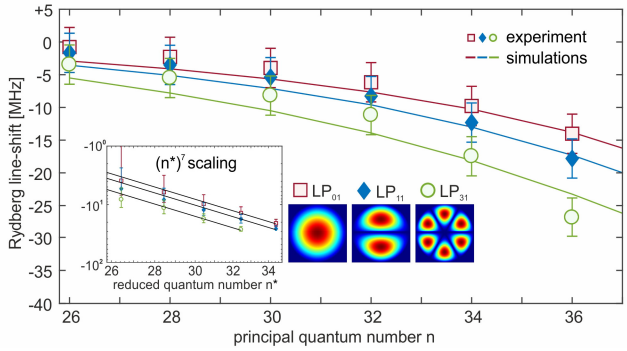

Fig. 3. Rydberg line-shifts measured using three different probe modes for increasing principal quantum number n. The solid curves show the trends of the simulated line-shifts based on the electric field generated by a fractional adatom surface density $\theta(z_1) = 0.0115$ with $\theta'(z_1) = 6\ \mathrm{m}^{-1}$ (see text). Inset: the measured line-shifts fit the expected $(n^*)^7$ scaling behavior (black lines) for electric fields.

Interactions with the core wall, via Casimir-Polder potentials, can influence the system, but typically only at distances of a few 100s of nm [28]. In any case Casimir-Polder interactions cannot explain the slow drift in measured frequency-shift over timescales of several months [22]. We therefore consider the line-shifts to be caused solely by Stark shifts resulting from stray static electric fields originating, for example, from charges or the dipole moments of adsorbed atoms [29]. The potentially strong effect of charges on a thermal Rydberg vapor has recently been investigated [21]. In analogy with Rydberg-Rydberg interactions, the density of charges created by ionization scales with the Rydberg density and hence is expected to be small in the PCF system. To test the potential influence of ions on the results, the measurements were repeated while setting the probe powers to half and twice their values (not shown), resulting in different Rydberg state populations. The difference in the measured shifts was comparatively small (0.68 MHz averaged over all modes at $n = 32$), suggesting that the ion creation rate is very low, i.e., that the surface density of ions on the core wall is negligible. This means that adsorbed atoms are the most likely cause of the electric fields, as we now discuss in more detail.

When a glass surface is exposed to an alkali atmosphere, atoms will adsorb onto it until the rates of adsorption and desorption are equal. It is known that these adsorbed atoms create stray electric fields in the vicinity of the adsorbing surface [29,30], as a consequence of partial electron charge transfer from the alkali to the SiO_2 surface, resulting in a dipole moment. Following the calculations in [30] we estimate the dipole moment for Cs on quartz to be $d_0 \approx 13$ D per adsorbed atom. The amount of atoms on the surface can be expressed by the fractional surface density of adatoms $\theta = \sigma_a/\sigma_0$, where σ_a is the surface density of adsorbed atoms and $\sigma_0 \sim 2 \times 10^6\ \mu\mathrm{m}^{-2}$ the estimated value for a close-packed monolayer [31]. The reported values for θ vary strongly but are found experimentally to lie in the range 10^{-4} to 1 [30-32]. Since the average distance between adatoms is small compared to the core dimensions it is valid to model them by a homogeneous dipole density on the core walls (Fig. 4 a). In our model this density can be constant or vary along the axial direction of the fiber as shown in Fig. 4 b. Such axial variations may result from the very slow diffusion rates of atoms along the core – typical filling times can be as long as several months.

To calculate the resulting electric field in the hollow-core region, we assume a fractional surface density of adatoms θ on the hexagonal core surface. In Fig. 4 c the core geometry considered by our model (indicated by the orange line) is compared to a scanning electron micrograph of the investigated kagomé-PCF. To model the effects of a changing adatom density along the fiber we assume that θ varies with z, i.e., $\theta(z_1 + dz) = \theta(z_1) + \theta'(z_1)dz$, where z_1 is an arbitrary position along the fiber. The inhomogeneously broadened Rydberg line-shifts will be determined not only by the radial variation in electric field, but also by non-zero values of $\theta'(z_1)$, which will give rise to an axial component of electric field.

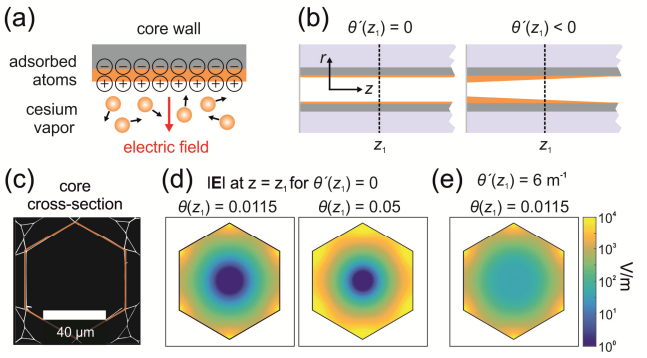

Fig. 4. (a) Radial electric field originating from dipoles of Cs atoms adsorbed on the core wall. (b) Adatom density in the vicinity of $z = z_1$. Left: if the filling time is long enough the fraction surface density of adatoms will be constant along the fiber. Right: for shorter filling times θ will depend on z. (c) Comparison of the core geometry considered by the adatom model (orange line) to a scanning electron micrograph of the investigated kagomé-PCF. (d) Modulus of the electric field over the core cross-section at $z = z_1$ for $\theta'(z_1) = 0; \theta(z_1) = 0.0115$ (left) and $\theta(z_1) = 0.05$ (right). (e) Modulus of the electric field (at $z = z_1$ for $\theta(z_1) = 0.0115$ and $\theta'(z_1) = 6\ \mathrm{m}^{-1}$. Here the z-dependence of θ creates an additional non-zero axial electric field component.

To extract the mean values of θ and θ' in the experiment we simulated the frequency shift using optical Bloch equations to model the coupling between the four-level atomic system and the excitation light fields (Fig. 1 c). Since the experiment is at ambient temperature, the thermal motion of the atoms is implemented by Doppler-shifts and mode dependent transit-times. The coupling strength of each transition is given by the intensity pattern of the corresponding excitation light field. The transverse intensity profiles of the LP_{01}, LP_{11} and LP_{31} modes in the core were calculated using the capillary approximation [33] (Fig. 2, lower row), and calibrated using the experimentally-measured power in each mode.

Due to the low Cs vapor density and low fiber loss the change in signal along the fiber is small and can be neglected. The signal will be generated where the vapor density is highest, i.e., predominantly in the regions close to the fiber ends. We evaluated the atomic response assuming an equivalent average electric field

distribution along the fiber. The core was sampled by a grid of points with 0.1 μm spacing. At each point the atomic response was calculated using the values of the local excitation and probe intensity and the static electric field. The full spectroscopic signal was then calculated by summing over all the grid-points. To extract the Rydberg line-shift from the simulated spectra, we used the same fitting procedure as in the experiment.

In Fig. 4 d the distribution of |**E**| over the core at arbitrary position $z = z_1$ is plotted for $\theta(z_1) = 0.0115$ (left) and $\theta(z_1) = 0.05$ (right) with $\theta'(z_1) = 0$. Radially pointing, |**E**| falls off rapidly with distance from the core wall, reaching zero on-axis. If $\theta'(z_1) \neq 0$, small z-components of electric field appear on-axis, as shown in Fig. 4 e for $\theta(z_1) = 0.0115$ and $\theta'(z_1) = 6\ \mathrm{m}^{-1}$. The solid curves in Fig. 3 plot the simulated electric field in this case for several different Rydberg orders. The simulated adatom density lies well within the range of values previously reported [30-32]. Calculations of diffusion along the fiber, assuming constant Cs-atom density at each end, show that a gradient of $6\ \mathrm{m}^{-1}$ corresponds to a penetration length of ~2.5 mm into the 8-cm-long fiber, with vanishing Cs density towards fiber middle. While this accords with our observation of very long filling times, the estimated value for the gradient seems exaggerated. However, the results would be very similar if the adatom density varied azimuthally around the core, when the broken symmetry would allow the fields to extend further into the core. In the real system we would expect the response to be a combination of both these effects, i.e., that our value for the adatom gradient is an upper limit.

Clearly, the closer the probed atoms are to the core wall the stronger is the adatom-generated electric field. On the other hand, the frequency shift of the atoms probed by modes that peak in the core center (for example, the LP_{01} mode) is dominated by the adatom gradient. This allows us to explain the results previously reported in [22], in which the observed Rydberg line-shift probed by the LP_{01} mode in a Cs-filled HC-PCF was drastically reduced after a very long filling time. If the density of adatoms is nearly constant along the fiber, the field components originating from the adatom gradient would vanish.

Conclusions. Selective launching of probe light into different guided modes in a HC-PCF filled with Rydberg atoms allows the spatial distribution of stray dc electric fields to be probed. These fields are caused by the dipole moment of Cs atoms adsorbed onto the glass wall of the hollow core. Comparison of experimental findings with simulations suggest that the mean fractional surface density of adatoms on the core-wall is 0.0115, with an average gradient along the fiber axis of $6\ \mathrm{m}^{-1}$. Analysis also indicates that the non-zero fields in the vicinity of the core center are caused by variations in adatom density along the fiber, which are the result of incomplete filling of the hollow-core PCF with Cs vapor. This explains previous observations [22], where the line-shifts were found to greatly reduce after long filling times, when the adatom density is expected to be uniform along the fiber. The use of waveguide modes and Rydberg atoms provides a unique means of quantitatively probing the dc electric field distribution inside a hollow-core PCF and will be of great help in electric-field-sensitive spectroscopy.

Funding. Deutsche Forschungsgemeinschaft (DFG), LO 1657/6-1; European Union H2020 FET Proactive project RySQ (Grant No. 640378).

References

1. M. Fleischhauer, A. Imamoglu, and J. P. Marangos, Rev. Mod. Phys. **77**, 633 (2005)
2. P. St.J. Russell, J. Lightwave Technol. **24**, 4729 (2006).
3. Y. Y. Wang, N. V. Wheeler, F. Couny, P. J. Roberts, and F. Benabid, Opt. Lett. **36**, 669 (2011).
4. F. Benabid, F. Couny, J. C. Knight, T. A. Birks, and P. St.J. Russell, Nature **434**, 488 (2005).
5. M. Bajcsy, S. Hofferberth, V. Balic, T. Peyronel, M. Hafezi, A. S. Zibrov, V. Vuletic, and M. D. Lukin, Phys. Rev. Lett. **102**, 203902 (2009).
6. C. Perrella, P. S. Light, J. D. Anstie, F. Benabid, T. M. Stace, A. G. White, and A. N. Luiten, Phys. Rev. A **88**, 013819 (2013).
7. V. Venkataraman, K. Saha, and A. L. Gaeta, Nat Photon **7**, 138 (2013).
8. M. R. Sprague, P. S. Michelberger, T. F. M. Champion, D. G. England, J. Nunn, X.-M. Jin, W. S. Kolthammer, A. Abdolvand, P. St. J. Russell and I. A. Walmsley, Nat Photon **8**, 287 (2014).
9. U. Vogl, C. Peuntinger, N. Y. Joly, P. St.J. Russell, C. Marquardt, and G. Leuchs, Opt. Express **22**, 29375 (2014).
10. K. T. Kaczmarek, D. J. Saunders, M. R. Sprague, W. S. Kolthammer, A. Feizpour, P. M. Ledingham, B. Brecht, E. Poem, I. A. Walmsley, and J. Nunn, Opt. Lett. **40**, 5582 (2015).
11. P. S. Donvalkar, S. Ramelow, S. Clemmen, and A. L. Gaeta, Opt. Lett. **40**, 5379 (2015).
12. H. Fan, S. Kumar, J. Sedlacek, H. Kübler, S. Karimkashi and J. P. Shaffer, J. Phys. B: At. Mol. Opt. Phys. **48**, *202001* (2015).
13. C. G. Wade, N. Šibalić, N. R. de Melo, J. M. Kondo, C. S. Adams and K. J. Weatherill, Nat Photon **11**, 40 (2017).
14. J. D. Pritchard, K. J. Weatherill, and C. S. Adams, Annual Review of Cold Atoms and Molecules Volume 1 p. 301 (2013)
15. D. Paredes-Barato and C. S. Adams, Phys. Rev. Lett. **112**, 040501 (2014).
16. H. Gorniaczyk, C. Tresp, J. Schmidt, H. Fedder, and S. Hofferberth, Phys. Rev. Lett. **113**, 053601 (2014).
17. J. Honer, R. Löw, H. Weimer, T. Pfau, and H. P. Büchler, Phys. Rev. Lett. **107**, 093601 (2011).
18. T. Baluktsian, B. Huber, R. Löw, and T. Pfau, Phys. Rev. Lett. **110**, 123001 (2013).
19. A. Urvoy, F. Ripka, I. Lesanovsky, D. Booth, J. P. Shaffer, T. Pfau, and R. Löw, Phys. Rev. Lett. **114**, 203002 (2015).
20. C. Carr, R. Ritter, C. G. Wade, C. S. Adams, and K. J. Weatherill, Phys. Rev. Lett. **111**, 113901 (2013).
21. D. Weller, A. Urvoy, A. Rico, R. Löw, and H. Kübler, Phys. Rev. A **94**, 063820 (2016).
22. G. Epple, K. S. Kleinbach, T. G. Euser, N. Y. Joly, T. Pfau, P. St.J. Russell, and R. Löw, Nature Communications **5**, 4132 (2014).
23. R. Löw, H. Weimer, J. Nipper, J.B. Balewski, B. Butscher, H.P. Büchler and T. Pfau, J. Phys. B: At. Mol. Opt. Phys. **45**, 113001 (2012).
24. T. G. Euser, G. Whyte, M. Scharrer, J. S. Y. Chen, A. Abdolvand, J. Nold, C. F. Kaminski, and P. St.J. Russell, Opt. Express **16**, 17972 (2008).
25. C.-J. Lorenzen and K. Niemax, Zeitschrift für Physik A Atoms and Nuclei **315**, 127 (1984).
26. S. Gu, S. Gong, B. Liu, J. Wang, Z. Dai, T. Lei and B. Li, J. Phys. B: At. Mol. Opt. Phys. **30**, 467 (1997).
27. C. Veit, G. Epple, H. Kübler, T. G. Euser, P. St. J. Russell and R Löw, J. Phys. B: At. Mol. Opt. Phys. **49**, 134005 (2016).
28. J. A. Crosse, S. Å. Ellingsen, K. Clements, S. Y. Buhmann, and S. Scheel, Phys. Rev. A **82**, 010901 (2010).
29. J. M. McGuirk, D. M. Harber, J. M. Obrecht, and E. A. Cornell, Phys. Rev. A **69**, 062905 (2004).
30. J. A. Sedlacek, E. Kim, S. T. Rittenhouse, P. F. Weck, H. R. Sadeghpour, and J. P. Shaffer, Phys. Rev. Lett. **116**, 133201 (2016).
31. M. A. Bouchiat, J. Guéna, P. Jacquier, M. Lintz, and A. V. Papoyan, Applied Physics B **68**, 1109 (1999).
32. H. N. de Freitas, M. Oria, and M. Chevrollier, Applied Physics B **75**, 703 (2002).
33. M. A. Finger, N. Y. Joly, T. Weiss, and P. St.J. Russell, Opt. Lett. **39**, 821 (2014)

References Full

1. M. Fleischhauer, A. Imamoglu, and J. P. Marangos, "Electromagneticallyinduced transparency: Optics in coherent media," Rev. Mod. Phys. **77**, 633 (2005)
2. P. St.J. Russell, "Photonic-Crystal Fibers," J. Lightwave Technol. **24**, 4729–4749 (2006).
3. Y. Y. Wang, N. V. Wheeler, F. Couny, P. J. Roberts, and F. Benabid, "Low loss broadband transmission in hypocycloid-core Kagome hollow-core photonic crystal fiber," Opt. Lett. **36**, 669–671 (2011).
4. F. Benabid, F. Couny, J. C. Knight, T. A. Birks, and P. St.J. Russell, "Compact, stable and efficient all-fibre gas cells using hollow-core photonic crystal fibres," Nature **434**, 488–491 (2005).
5. M. Bajcsy, S. Hofferberth, V. Balic, T. Peyronel, M. Hafezi, A. S. Zibrov, V. Vuletic, and M. D. Lukin, "Efficient All-Optical Switching Using Slow Light within a Hollow Fiber," Phys. Rev. Lett. **102**, 203902 (2009).
6. C. Perrella, P. S. Light, J. D. Anstie, F. Benabid, T. M. Stace, A. G. White, and A. N. Luiten, "High-efficiency cross-phase modulation in a gas-filled waveguide," Phys. Rev. A **88**, 013819 (2013).
7. V. Venkataraman, K. Saha, and A. L. Gaeta, "Phase modulation at the few-photon level for weak-nonlinearity-based quantum computing," Nat Photon **7**, 138–141 (2013).
8. M. R. Sprague, P. S. Michelberger, T. F. M. Champion, D. G. England, J. Nunn, X.-M. Jin, W. S. Kolthammer, A. Abdolvand, P. St. J. Russell and I. A. Walmsley, "Broadband single-photon-level memory in a hollow-core photonic crystal fibre," Nat Photon **8**, 287–291 (2014).
9. U. Vogl, C. Peuntinger, N. Y. Joly, P. St.J. Russell, C. Marquardt, and G. Leuchs, "Atomic mercury vapor inside a hollow-core photonic crystal fiber," Opt. Express **22**, 29375–29381 (2014).
10. K. T. Kaczmarek, D. J. Saunders, M. R. Sprague, W. S. Kolthammer, A. Feizpour, P. M. Ledingham, B. Brecht, E. Poem, I. A. Walmsley, and J. Nunn, "Ultrahigh and persistent optical depths of cesium in Kagomé-type hollow-core photonic crystal fibers," Opt. Lett. **40**, 5582–5585 (2015).
11. P. S. Donvalkar, S. Ramelow, S. Clemmen, and A. L. Gaeta, "Continuous generation of rubidium vapor in hollow-core photonic bandgap fibers," Opt. Lett. **40**, 5379–5382 (2015).
12. H. Fan, S. Kumar, J. Sedlacek, H. Kübler, S. Karimkashi and J. P. Shaffer, "Atom based RF electric field sensing," Journal of Physics B: Atomic, Molecular and Optical Physics **48**, *202001* (2015).
13. C. G. Wade, N. Šibalić, N. R. de Melo, J. M. Kondo, C. S. Adams and K. J. Weatherill, "Real-time near-field terahertz imaging with atomic optical fluorescence," Nat Photon **11**, 40–43 (2017).
14. J. D. Pritchard, K. J. Weatherill, and C. S. Adams, "Nonlinear optics using cold Rydberg atoms," in *Annual Review of Cold Atoms and Molecules*, Annual Review of Cold Atoms and Molecules Volume 1, pp. 301–350 (2013).
15. D. Paredes-Barato and C. S. Adams, "All-Optical Quantum Information Processing Using Rydberg Gates," Phys. Rev. Lett. **112**, 040501 (2014).
16. H. Gorniaczyk, C. Tresp, J. Schmidt, H. Fedder, and S. Hofferberth, "Single-Photon Transistor Mediated by Interstate Rydberg Interactions," Phys. Rev. Lett. **113**, 053601 (2014).
17. J. Honer, R. Löw, H. Weimer, T. Pfau, and H. P. Büchler, "Artificial Atoms Can Do More Than Atoms: Deterministic Single Photon Subtraction from Arbitrary Light Fields," Phys. Rev. Lett. **107**, 093601 (2011).
18. T. Baluktsian, B. Huber, R. Löw, and T. Pfau, "Evidence for Strong van der Waals Type Rydberg-Rydberg Interaction in a Thermal Vapor," Phys. Rev. Lett. **110**, 123001 (2013).
19. A. Urvoy, F. Ripka, I. Lesanovsky, D. Booth, J. P. Shaffer, T. Pfau, and R. Löw, "Strongly Correlated Growth of Rydberg Aggregates in a Vapor Cell," Phys. Rev. Lett. **114**, 203002 (2015).
20. C. Carr, R. Ritter, C. G. Wade, C. S. Adams, and K. J. Weatherill, "Nonequilibrium Phase Transition in a Dilute Rydberg Ensemble," Phys. Rev. Lett. **111**, 113901 (2013).
21. D. Weller, A. Urvoy, A. Rico, R. Löw, and H. Kübler, "Charge-induced optical bistability in thermal Rydberg vapor," Phys. Rev. A **94**, 063820 (2016).
22. G. Epple, K. S. Kleinbach, T. G. Euser, N. Y. Joly, T. Pfau, P. St.J. Russell, and R. Löw, "Rydberg atoms in hollow-core photonic crystal fibres," Nature Communications **5**, 4132 (2014).
23. R. Löw, H. Weimer, J. Nipper, J.B. Balewski, B. Butscher, H.P. Büchler and T. Pfau, "An experimental and theoretical guide to strongly interacting Rydberg gases," Journal of Physics B: Atomic, Molecular and Optical Physics **45**, 113001 (2012).
24. T. G. Euser, G. Whyte, M. Scharrer, J. S. Y. Chen, A. Abdolvand, J. Nold, C. F. Kaminski, and P. St.J. Russell, "Dynamic control of higher-order modes in hollow-core photonic crystal fibers," Opt. Express **16**, 17972–17981 (2008).
25. C.-J. Lorenzen and K. Niemax, "Precise quantum defects of nS, nP and nD Levels in Cs I," Zeitschrift für Physik A Atoms and Nuclei **315**, 127–133 (1984).
26. S. Gu, S. Gong, B. Liu, J. Wang, Z. Dai, T. Lei and B. Li, "Experimental study of caesium atom $n\,^2P_{3/2}$ Rydberg state polarizabilities by Doppler-free resonantly enhanced two-photon technique," Journal of Physics B: Atomic, Molecular and Optical Physics **30**, 467 (1997).
27. C. Veit, G. Epple, H. Kübler, T. G. Euser, P. St. J. Russell and R Löw, "RF-dressed Rydberg atoms in hollow-core fibres," Journal of Physics B: Atomic, Molecular and Optical Physics **49**, 134005 (2016).
28. J. A. Crosse, S. Å. Ellingsen, K. Clements, S. Y. Buhmann, and S. Scheel, "Thermal Casimir-Polder shifts in Rydberg atoms near metallic surfaces," Phys. Rev. A **82**, 010901 (2010).
29. J. M. McGuirk, D. M. Harber, J. M. Obrecht, and E. A. Cornell, "Alkali-metal adsorbate polarization on conducting and insulating surfaces probed with Bose-Einstein condensates," Phys. Rev. A **69**, 062905 (2004).
30. J. A. Sedlacek, E. Kim, S. T. Rittenhouse, P. F. Weck, H. R. Sadeghpour, and J. P. Shaffer, "Electric Field Cancellation on Quartz by Rb Adsorbate-Induced Negative Electron Affinity," Phys. Rev. Lett. **116**, 133201 (2016).
31. M. A. Bouchiat, J. Guéna, P. Jacquier, M. Lintz, and A. V. Papoyan, "Electrical conductivity of glass and sapphire cells exposed to dry cesium vapor," Applied Physics B **68**, 1109–1116 (1999).
32. H. N. de Freitas, M. Oria, and M. Chevrollier, "Spectroscopy of cesium atoms adsorbing and desorbing at a dielectric surface," Applied Physics B **75**, 703–709 (2002).
33. M. A. Finger, N. Y. Joly, T. Weiss, and P. St.J. Russell, "Accuracy of the capillary approximation for gas-filled kagomé-style photonic crystal fibers," Opt. Lett. **39**, 821–824 (2014).